

Article

Advanced Design for Experimental Optimisation of Physico-Mechanical Characteristics of Sustainable Local Hemp Concrete

Laurentiu Adam¹, Loredana Judele¹, Iuliana Motrescu² , Ion Rusu³, Daniel Lepadatu^{1,3,*} 
and Roxana Dana Bucur⁴

- ¹ Faculty of Civil Engineering and Building Services, Gheorghe Asachi Technical University of Iasi, 700050 Iasi, Romania; laurentiu.adam@student.tuiasi.ro (L.A.); loredana-emanuela.judele@academic.tuiasi.ro (L.J.)
- ² Department of Exact Sciences & Research Institute for Agriculture and Environment, “Ion Ionescu de la Brad” Iasi University of Life Sciences, 700490 Iasi, Romania
- ³ Transport Infrastructure Engineering Department, Faculty of Urban Planning and Architecture, Technical University of Moldova, 2028 Chisinau, Moldova
- ⁴ Livestock Building Department, “Ion Ionescu de la Brad” Iasi University of Life Sciences, 700490 Iasi, Romania
- * Correspondence: daniel.lepadatu@iit.utm.md

Abstract: The meaning of technological progress is to produce economic development and to increase the level of personal comfort. Sustainability can only be achieved if, at the microsystem level as well as at the macrosystem level, the secondary effects of the activities undertaken by people on the environment are in a state of neutrality compared to the impact they can produce on natural conditions. This neutrality can be intrinsic or can be achieved through coercive and compensatory measures. If we take into account the production of carbon dioxide that accompanies a product from the stages of conceptualisation, design, procurement of materials, execution, operation, maintenance, decommissioning and recycling the waste produced at the end of use, then nothing can be sustainable in pure form. Nevertheless, there are products whose production, both as a raw material and as a technological process, can be neutral in terms of carbon emissions. Moreover, they can even become carbon negative over time. This is also the case with eco-sustainable hemp concrete, whose capacity to absorb carbon dioxide starts from the growth phase of the plant from which the raw material is obtained and continues throughout the existence of the constructed buildings. Not only does it absorb carbon dioxide, but it also stores it for a period of at least 50 years as long as the construction is guaranteed, being at the same time completely recyclable. However, in order to obtain an optimal mixture from the point of view of raw material consumption, represented by industrial hemp wood chips and the binder based on lime and cement, multiple experiments are necessary. The study presented in this work is based on the use of an advanced method of experimental planning (design of experiments method), which makes possible the correlation between the values obtained experimentally and the algorithm that generated the matrix arrangement of the quantities of materials used in the recipes. This approach helps to create the necessary framework for parametric optimisation with a small number of trials. Thus, it is possible to obtain the mathematical law valid within the minimum and maximum limits of the studied domain that defines the characteristics of the material and allows the achievement of optimisation. The material is thus designed to satisfy the maximum thermal insulation requirements that it can achieve depending on a certain minimum admissible compressive strength.



Citation: Adam, L.; Judele, L.; Motrescu, I.; Rusu, I.; Lepadatu, D.; Bucur, R.D. Advanced Design for Experimental Optimisation of Physico-Mechanical Characteristics of Sustainable Local Hemp Concrete. *Sustainability* **2023**, *15*, 8484. <https://doi.org/10.3390/su15118484>

Academic Editor: Marijana Hadzima-Nyarko

Received: 31 March 2023

Revised: 8 May 2023

Accepted: 19 May 2023

Published: 23 May 2023



Copyright: © 2023 by the authors. Licensee MDPI, Basel, Switzerland. This article is an open access article distributed under the terms and conditions of the Creative Commons Attribution (CC BY) license (<https://creativecommons.org/licenses/by/4.0/>).

Keywords: local hemp concrete; design of experiments method; advanced optimisation

1. Introduction

More than 36 years have passed since the first officially mentioned use of hemp concrete [1]. Studies on this bio-composite material [2,3] are continuously developing,

so there are important works presenting applications [4–8] of this material in the field of construction [9–12]. It can be used to build insulating walls using self-supporting bricks or as infill in lost formwork and for the plastering layer both in new construction and the renovation of traditional buildings. It is often used to insulate floors, walls, and roofs. It is also used for casting leveling layers due to its low specific weight. Due to the natural porosity of hemp, it can be used successfully in sound-absorbing insulation or for vibration damping. By modifying the grain size and using automated mixing technologies, constructions can be obtained using 3D printers. However, the versatility of this eco-sustainable material [13–16] continues to be surprising, with the possibility of its use in more and more industries [17–19].

Previous studies have shown the thermo-mechanical performance of hemp concrete [20–26] with the limitations of being a non-structural material [27–30], but at the same time, it excels when it comes to heat transfer and the thermo-regulating capacity of ambient humidity, which makes it recognised as a very good thermal insulation material with a decisive role in increasing the hygro-thermal performance of sustainable constructions [31–33]. The fact that it is obtained from natural sources as a by-product of agricultural activities qualifies it in the race for the best products with potential in the circular economy [34] while contributing to the reduction of carbon emissions [35–38]. Today's society, in the midst of the changes imposed by climate change, is forced to adopt a different way of life. It has to learn to repress its previously acquired routines and change its habits in order to develop new, environmentally friendly reflexes. Despite the benefits that hemp concrete and hemp, in general, can offer, the media coverage, adoption, and application of technological solutions that implement this plant-based concrete are mainly reduced by the reluctance created due to the industry producing dedicated and traditional conventional building materials, which facilitates the application of easy-to-use installation technologies by anyone with minimal skills. The placing of hemp concrete, although it has various technological variants [39,40], involves greater attention and an additional workload both for the mixture and installation, as the material has a different consistency from any type of mortar mixture or conventional concrete.

Hemp concrete mixtures are differentiated by the construction element for which the mix is made. Depending on the ratio of hemp, binder, admixtures, and water used, selective thermo-mechanical properties can be obtained for both the heat transfer coefficient and compressive strength. The possibility to design the material according to the energy efficiency requirements, the advantage of being obtained from sustainable raw materials, and the ability to be used at the end life cycle as recycled aggregate concrete [41,42] have contributed to our attempt to optimise the physico-mechanical performances using an advanced method of conducting experiments. The method is based on statistical computation used both for the design of laboratory trials and for the interpretation of test results, hereafter referred to as design of experiment (DoE). This is an advanced experimental design technique discovered by Sir R. A. Fisher in the 1920s, an English statistician who introduced it in Europe to the major prestigious universities with which he was associated through the book *The Design of Experiments* [43,44], published in its first edition in 1935. This book was based on a first work by the author in 1925 [44], which was in fact a laboratory guide presenting this revolutionary method. Used in agriculture for the first time by Fisher, the method was developed by statisticians Box and Wilson [45] in the era of the first industrial revolution between 1950 and 1970, who introduced the concept of response surface modelling for non-linear phenomena and helped users to optimise industrial processes, especially in the chemical industry at that time, by identifying the combination of parameters that could influence a process so as to obtain a desired optimum on a physical or mechanical characteristic of the process.

The second industrial revolution between the 1970s and 1990s was mentored by Taguchi [46], a Japanese engineer who introduced the concept of quality quantified by S/N (signal-to-noise ratio) and the robustness of industrial processes by decreasing the variability of the multiple responses of such a complex system. This industrial era, also

known as the quality revolution, contributed to the development and consolidation of robust products that had, as an essential characteristic, greater durability over time and, as a result, much-improved customer satisfaction.

2. Materials and Methods

2.1. Materials used to Make the Composition of Hemp Concrete

The basic material used to obtain the specimens was hemp shive (Figure 1), with a particle size between 0 and 35 mm and a bulk density of 100 kg/m³.



Figure 1. Hemp shive.

A mineral binder was used that was composed of a mixture of hydrated lime, having the characteristics of Table 1, and Portland cement, having the chemical composition listed in Table 2 and the physical characteristics stated in Table 3.

Table 1. Components of hydrated lime.

Components	Unit Measurements	Values
CaO + MgO	%	≥80
Free lime Ca (OH) ₂	%	≥65
MgO	%	≤5
CO ₂	%	≤15
SO ₃	%	≤2
Free water	%	≤2
Air content	%	≤12
Bulk density	kg/m ³	625

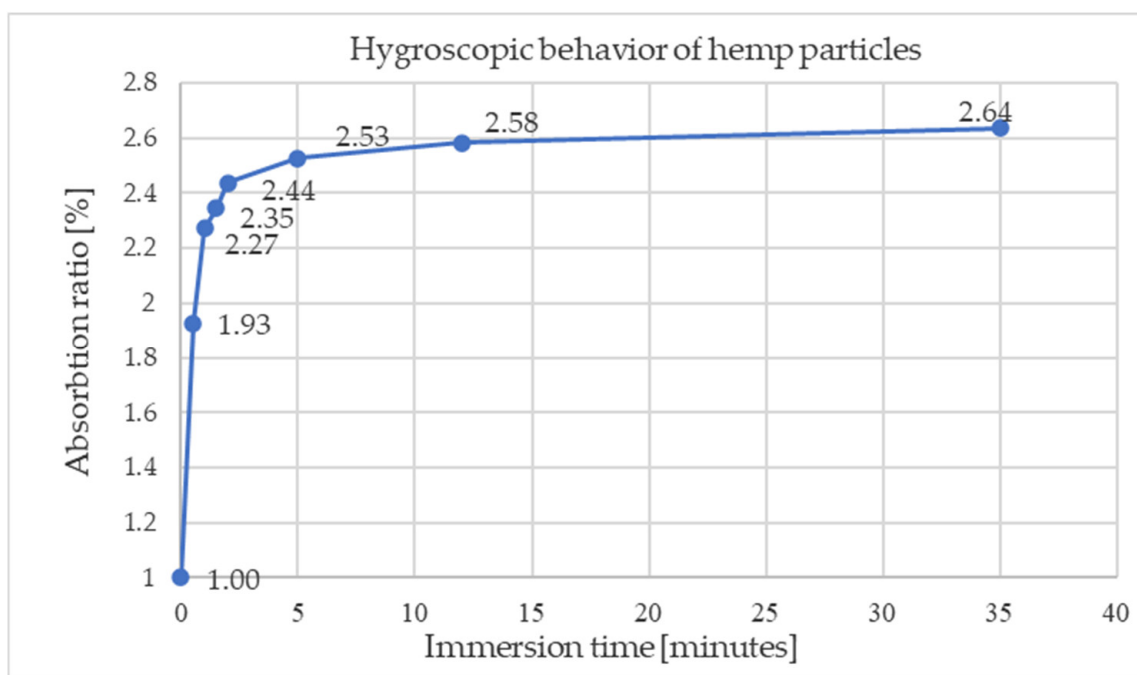
Table 2. Chemical composition of Portland cement.

Components	Unit Measurements	Values
SO ₃	%	21.7
Al ₂ O ₃	%	7.3
Fe ₂ O ₃	%	3.4
CaO	%	64.1
MgO	%	1.7
TiO ₂	%	0.2
Na ₂ O	%	0.5
K ₂ O	%	0.8
Insoluble	%	0.3

Table 3. Characteristics of Portland cement.

Characteristics	Unit Measurements	Values
Clinker (K) content	%	65 ÷ 79
Furnace slag (S) and chalk (LL) content	%	21 ÷ 35
Sulfate content in the form of SO ₃	%	≤3.5
Standard compressive strength	MPa	42.5 ÷ 62.5
Expansion stability	mm	≤3
Bulk density	kg/m ³	1450

Sodium silicate (glass water) solution, with a concentration of 35–40%, was added to the mixture in a proportion of 5% by mass of the water used to hydrate the mineral binders. The role of this compound was to work as an additive to enhance the binding speed, resulting in the rapid hardening of the hemp concrete and influencing the hydration of the Portland cement's hydraulic binder [47]. The strong hygroscopic character of hemp shive (Figure 2) must be reduced to avoid the absorption of water necessary for binder hydration. Thus, in the mixing technology, before adding the binder mix, the hemp particles are hydrated with an amount of water equal to the mass of the dry hemp.

**Figure 2.** Hygroscopic behaviour of the hemp shive.

2.2. Making Specimens

The following method (Figure 3) was used to make fresh hemp concrete mix. First, a premixed binder obtained from hydrated lime and Portland cement was added according to the quantities specified in the mixture, and an amount of water equal to the dry mass of the hemp used was added to the hemp traces that were hydrated. The materials were then mixed, and a premix of sodium silicate was added to the water used to hydrate the binder mixture. The binder mixture was then added to the hemp traces and was mixed until a homogeneous solution was obtained. The sodium silicate water solution was then added to this solution and homogenised. We then poured the fresh hemp concrete into a 15 cm cube shape. Hemp concrete samples (Figure 4) were cast according to EN 12390-1 [47] and EN 12390-3 [48].

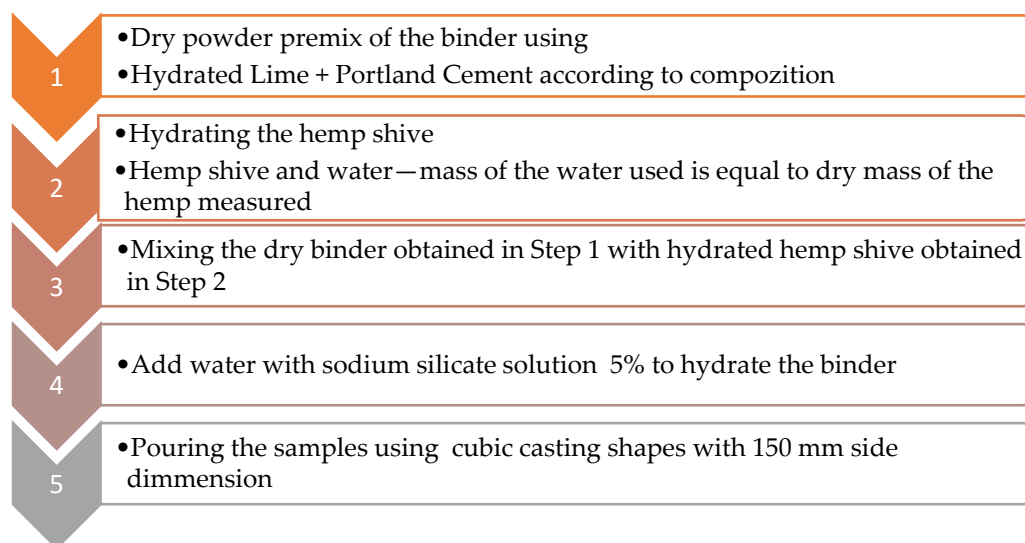


Figure 3. Method used to obtain hempcrete mixture—flow chart.



Figure 4. Cubic samples.

2.3. Design of Experiment Method

The introduction of these techniques required the use of mathematical concepts such as matrices with special properties (rotatability, D optimal, A optimal) that brought users maximum satisfaction with minimum resources [49–51]. There are many fields where this method has been successfully applied, including agriculture [52,53], materials science [54,55], environment [56,57], process optimisation [58,59], sustainable building construction [14,15], etc. Overall, it can be said that the experimental planning method is able to solve processes/phenomena of the black box type shown in Figure 5 that depend on a series of known/controllable input factors, X_i , and that can influence their output characteristics, Y_i , called output factors, being totally dependent on them. However, being a complex process/phenomenon that can only be modelled numerically/analytically under certain conditions and, therefore, with restrictions and assumptions, it is affected by other unknown factors called uncontrollable or noise factors ε [43–46], which are systematic errors.

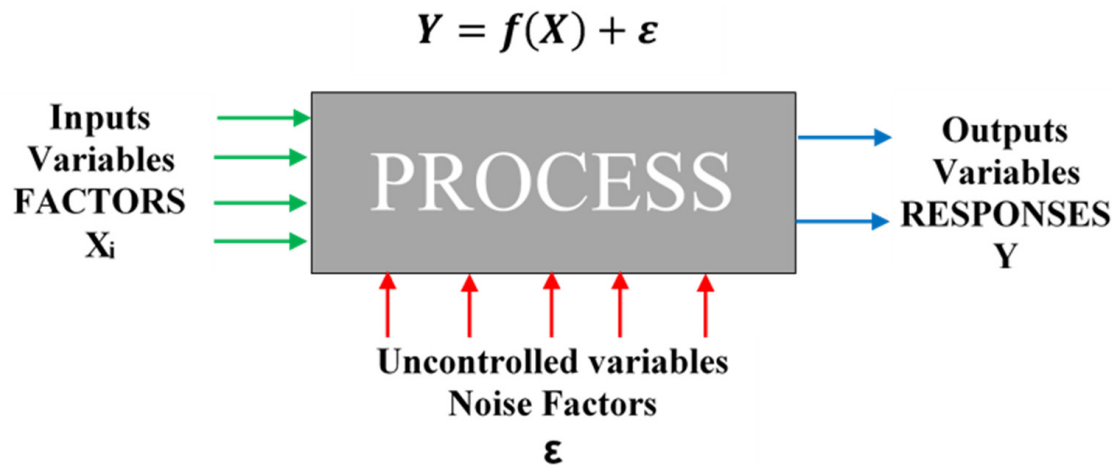


Figure 5. Black box for any process (in green—input variables, in blue—output variables, and in red—noise factors).

The mathematical equation that links all these factors is of the form (Equation (1))

$$Y = f(X) + \varepsilon \quad (1)$$

In general, the mathematical equation for multiple linear regression [49] is given by

$$Y_i = \beta_0 + \sum \beta_i x_i + \sum \beta_i x_i x_j + \sum \beta_i x_i x_j x_k + \varepsilon \quad (2)$$

where Y_i represents the dependent variable or response; β_0 represents the intercept; x_i, x_j, x_k are independent variables or factors; β_i is the regression coefficient; and ε is the disturbance error.

The aim of the work was to optimise the thermo-mechanical performance of an ecological, sustainable concrete based on hemp and a mineral binder based on hydrated lime. Using the advanced DoE method, based on previous studies and laboratory experiments, the results obtained from the experimental design were analysed, where 16 specimens were made according to the factorial design. SEM images were analysed, and following the application of mathematical regression equations, the recipes for which the targeted output variables Y_1 , the heat transfer coefficient, and Y_2 , the compressive strength, were validated and analysed to justify the importance and usefulness of the method used.

The use of the methods involves going through several steps, such as defining the objective, setting the parameters/variable factors for the study, choosing the experimental design according to the objective, performing the experiments and testing the samples on different samples, executing a statistical analysis of the experimental data, setting the regression equations, optimising the physicommechanical characteristics, and experimentally validating the numerical values obtained. Thus, Table 4 shows the variable factors and their magnitudes. The maximum and minimum limits were chosen to satisfy a response surface targeted by the expected experimental values. For example, the lower limit for hydrating lime is 164 g, and the upper limit is 238 g. These values correspond to an output-dependent magnitude, which was quantified according to the values obtained for heat transfer and compressive strength.

Therefore, the experimental design chosen to generate the parameter for the mixtures and the conduct of laboratory trials is presented in Table 5. The minimum and maximum values for the given composites were based on previous studies. Quantities are given by mass because each parameter has different densities, and measurement by volume would not have made it possible to add water and the silicate solution according to the minimum ratio of water to cement or water to sodium silicate.

Table 4. Range of variables and their coded form.

Variable	Lower Limit		Upper Limit	
	Coded Value	Real Value (Grams)	Coded Value	Real Value (Grams)
Lime (X_1)	−1	164	1	238
Cement (X_2)	−1	55	1	170
Water (X_3)	−1	219	1	408
Silicate (X_4)	−1	11	1	21

Table 5. Full factorial plan for mixtures design of experiments.

Samples	Hydrated Lime (Grams)	Cement (Grams)	Water (Grams)	Silicate (Grams)
1	164	55	219	11
2	238	55	219	11
3	164	170	219	11
4	238	170	219	11
5	164	55	408	11
6	238	55	408	11
7	164	170	408	11
8	238	170	408	11
9	164	55	219	21
10	238	55	219	21
11	164	170	219	21
12	238	170	219	21
13	164	55	408	21
14	238	55	408	21
15	164	170	408	21
16	238	170	408	21

After casting the samples according to the factorial plan presented above, the experiments were conducted to test the samples for the heat transfer coefficient using ISOMET 2114 [60], a piece of laboratory equipment for the measurement of the heat transfer properties of materials. This equipment is a hand-held meter for the direct measurement of heat transfer properties of a wide range of materials, including those considered insulating. It applies a dynamic measurement method, which allows a reduction in measurement time compared to steady-state measurement methods. The evaluation of thermal conductivity and volumetric heat capacity is based on temperature records sampled periodically as a function of time, provided that heat propagation takes place in an unbounded medium. The measurements were made after 28 days of curing time when the mass of the cubic samples remained constant. The measurement was made using a surface probe (Figure 6.) The values obtained for the heat transfer coefficient are summarised in Table 6.

Table 6. Experimental values obtained for the heat transfer coefficient.

Sample	Values W/m·K
1	0.1131
2	0.1121
3	0.1077
4	0.1021

For the compression test, the experimental values measured to determine the mechanical strength were made after 28 days of curing using a WAW-600E hydraulic press with a maximum load of 600 kN, presented in Figure 7. The measurements were taken according to EN 12390-3 [48].



Figure 6. Measurement for the heat transfer coefficient using ISOMET 2114 [60].



Figure 7. Compression test.

The values obtained from measurements made under laboratory conditions are presented in Table 7, together with the predicted values generated from the statistical calculations, for which the residual value for each of the compared values is provided.

The approximation grade of regression equations is given by R^2 , which indicates a very good approximation of the values. In order to optimise the physico-mechanical characteristics according to the configuration of the parameters, it is necessary to identify the combination of parameters (input factors) that satisfies the user's requirements for strength. Thus, mathematical optimisation helps us by using the regression equations obtained by the statistical method, and further on, we can identify the functions that satisfy those constraints.

The form of the mathematical regression function with an approximation degree of $R^2 = 0.93$ for conductivity (Y_1) is given by Equation (3).

$$\begin{aligned}
 Y_1 = & 3941.43 \cdot 10^{-4} - 12.39 \cdot 10^{-4} \cdot X_1 + 2.79 \cdot 10^{-4} \cdot X_2 - 8.499 \cdot 10^{-4} \cdot X_3 \\
 & - 89.820 \cdot 10^{-4} \cdot X_4 - 0.01 \cdot 10^{-4} \cdot X_1 X_2 \\
 & + 0.03 \cdot 10^{-4} \cdot X_1 X_3 + 0.4 \cdot 10^{-4} \cdot X_1 X_4 + 0.03 \cdot 10^{-4} \cdot X_2 X_3 \\
 & - 0.031 \cdot 10^{-4} \cdot X_2 X_4 + 0.13 \cdot 10^{-4} \cdot X_3 X_4
 \end{aligned} \quad (3)$$

Table 7. Observed, predicted, and residual values of compressive strength and conductivity.

	Conductivity— Y_1			Compressive Strength— Y_1		
	Observed	Predicted	Residual	Observed	Predicted	Residual
1	0.114	0.133	0.020	0.373	0.404	−0.032
2	0.123	0.117	−0.006	0.433	0.414	0.019
3	0.198	0.178	−0.020	0.762	0.783	−0.021
4	0.148	0.154	0.006	0.645	0.612	0.033
5	0.120	0.116	−0.004	0.308	0.347	−0.040
6	0.149	0.139	−0.009	0.477	0.425	0.052
7	0.216	0.220	0.004	1.091	1.000	0.092
8	0.226	0.236	0.009	0.792	0.896	−0.104
9	0.133	0.121	−0.012	0.450	0.397	0.053
10	0.136	0.134	−0.002	0.385	0.426	−0.041
11	0.119	0.130	0.012	0.711	0.712	−0.001
12	0.134	0.136	0.002	0.549	0.560	−0.011
13	0.132	0.128	−0.003	0.301	0.283	0.018
14	0.164	0.181	0.017	0.349	0.380	−0.031
15	0.193	0.197	0.003	0.802	0.872	−0.070
16	0.259	0.242	−0.017	0.870	0.788	0.083

The predicted values were obtained by regression with an error of 0.07%. The value of the regression coefficients for each parameter or combination of parameters indicates their magnitude on thermal conductivity.

The form of the mathematical regression function with an approximation degree of $R^2 = 0.95$ for the compressive strength (Y_2) is given by Equation (4).

$$\begin{aligned}
 Y_2 = & 3492.99 \cdot 10^{-4} - 0.45 \cdot 10^{-4} \cdot X_1 + 46.33 \cdot 10^{-4} \cdot X_2 - 14.56 \cdot 10^{-4} \\
 & \cdot X_3 + 47.05 \cdot 10^{-4} \cdot X_4 - 0.21 \cdot 10^{-4} \cdot X_1 X_2 \\
 & + 0.05 \cdot 10^{-4} \cdot X_1 X_3 + 0.26 \cdot 10^{-4} \cdot X_1 X_4 + 0.13 \cdot 10^{-4} \cdot X_2 X_3 \\
 & - 0.55 \cdot 10^{-4} \cdot X_2 X_4 - 0.3 \cdot 10^{-4} \cdot X_3 X_4
 \end{aligned} \quad (4)$$

After establishing the regression equations, we can conclude:

- The linear parts of the regression equations have positive terms, which indicates that at a maximum value of the objective function (thermal conductance or compression), the variables X_1 – X_4 will vary towards positive levels of the experimental domain;
- The coefficient of the negative interaction terms causes a decrease in the objective function when the variables X_1 and X_4 have opposite signs and produces an increase when they have the same sign. Using this equation produced thermal conductivity values for parameter configurations that maximise, minimise, or can achieve a desired value for the user depending on the needs.

3. Results and Discussion

3.1. Results Obtained for the Validation Samples

Validation of the experimental results for the heat transfer coefficient (Y_1) and compressive strength (Y_2) is presented in Table 8.

Table 8. Validation of physicommechanical characteristics of hemp concrete.

Sample	X_1	X_2	X_3	X_4	Y_1 (W/m ² *K)	Y_2 (MPa)
1	238	63.55	408	21	0.1131	0.115
2	238	122.31	408	21	0.1121	0.405
3	164	123	219	21	0.1077	0.494
4	164	170	295	11	0.1021	0.635

In this table, predicted values were presented using the mathematical Equations (3) and (4) obtained by regression and experimentally validated. These are the maximum values of the

physicomechanical characteristics with variations of the parameters X_1 — X_4 on the studied areas that can be found in Table 3. These quantities are part of the validation stage of the numerically predicted values by real experimental tests.

It can be seen from the values presented in the table that the optimisation of the thermo-mechanical performance of hemp concrete was aimed at improving the mechanical compressive strength and reducing the heat transfer coefficient. Sample number 4 meets both conditions, considering that for a maximum recorded compressive strength of 0.635 MPa, the heat transfer coefficient obtained is 0.1021 W/m²*K. Comparing the quantities of Portland cement used in the four compositions, it can be seen that they increase from sample 1 to sample 4; at the same time, the quantity of hydrated lime decreases from sample 1 to sample 4, and the quantity of water used for hydration also decreases. This variation of parameters, imposed by the DoE method, resulted in a binder matrix consisting of hydrated lime, Portland cement, and sodium silicate water solution, which bound the hemp particles at the contact points, resulting in a hemp concrete resembling a three-dimensional grid. While the amount of air entrained between the hemp particles enveloped by the binder matrix led to a reduction in the heat transfer coefficient, the binder matrix composition developed increased compressive strengths. The porosity of the binder matrix was reduced; instead, we are talking about a volume of entrained air at the macrosystem level. Thus, sample 4 acquired both superior insulating properties and increased compressive strength. The use of the design of experiments method allowed us a parametric one-criteria optimisation of the physico-mechanical characteristics of the concrete hemp by obtaining the combination that satisfies the user's needs for each desired response. This could not be done with classical methods by trial and error. Thus, the mathematical properties of the initial experimental design provided the user with a powerful planning, analysis and optimisation tool that, through a relatively small number of experimental trials, provided us with maximum information about the physico-mechanical characteristics of the concrete hemp, in addition to a mathematical function necessary and useful for the single-criteria parametric optimisation process.

Figure 8 shows the evolution of the mechanical performance of the compressive strength of all four specimens whose recipes were optimised based on mathematical regression. The load-displacement graph shows an improving trend starting with sample 1 and reaches the optimal values with sample 4. The stress-strain characteristic curve of specimen 4 describes the elastic behaviour, confirming the increase in mechanical performance obtained by the DoE optimisation method.

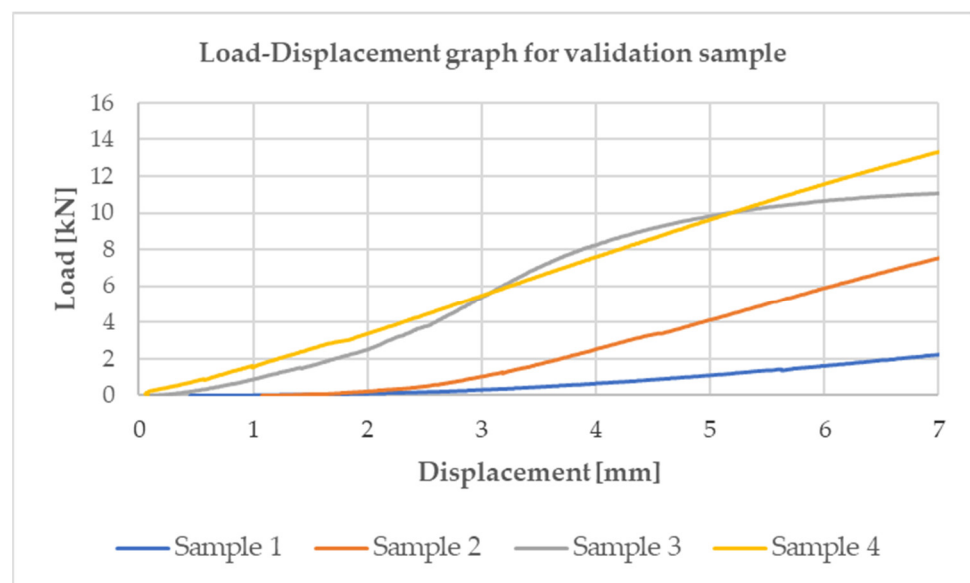


Figure 8. Compression test of validated samples.

3.2. Microimaging and Elemental Composition Analysis

Microimaging was performed on the fractured samples using a Quanta 450 scanning electron microscope (SEM) (FEI, Thermo Fisher Scientific, Hillsboro, OR, USA). The samples were put on aluminum stubs using carbon double tape. The electron microscope has a detector for energy dispersive X-ray spectroscopy (EDS) (EDAX, AMETEK Inc., Berwyn, PA, USA) that was used after imaging to determine the relative elemental composition of the samples.

All images from Figure 9 indicate that the appearance of the samples was quite homogeneous, showing that the composite mixture was already very well blended.

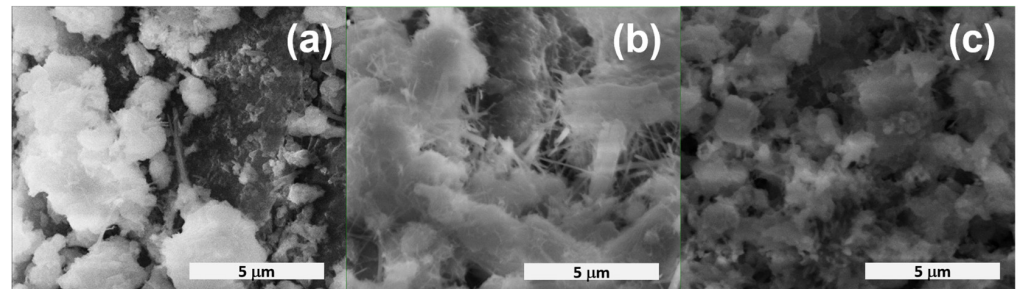


Figure 9. The samples under different magnifications: (a) sample 1, (b) sample 3, and (c) sample 10.

As can be seen in all the photos, silicate crystals predominate, and they consist of particles of several sizes, with sheet-like and polyhedral shapes tightly associated. It is easy to observe that they are larger crystals, even with the layered structure of crystal 1 in Figure 10, which has a length of approximately 12.9 µm. There are also crystals of about 10.3 µm length and 5.7 µm width (crystal 2) and smaller, with a length of about 7.8–9 µm (crystal 3) and even smaller.

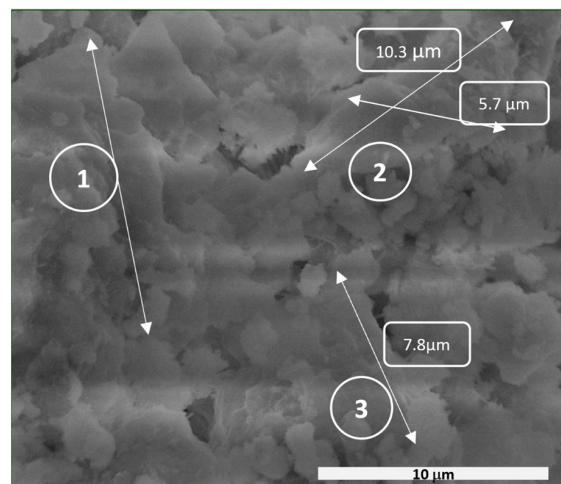


Figure 10. SEM image of the sample surface with an indication of (1) layered structure and ((2) and (3)) different sizes of crystals.

According to the SEM images, in all cases, the morphology of the processed samples does not change dramatically in terms of particle shapes and sizes or surface roughness with the modification of the quantities of the ingredients. The comparative analysis of the results of the samples indicates the highlighting of the shape and size of SiO₂ crystals from the added silicate as an initial ingredient, but also from the silicates present in the mineralogical composition of the cement.

Figure 11 demonstrates a uniformisation of the crystals in the sense that the sizes of the crystals have close values. There are no longer such large differences between crystal

lengths, nor between length and width, for the same crystal (the length is almost equal to the width, and they are about $4\ \mu\text{m}$). The crystals of very small size (crystals 1 in Figure 11) come from the added lime. It can be seen that their number has increased compared to sample 3, as the amount of lime has also increased.

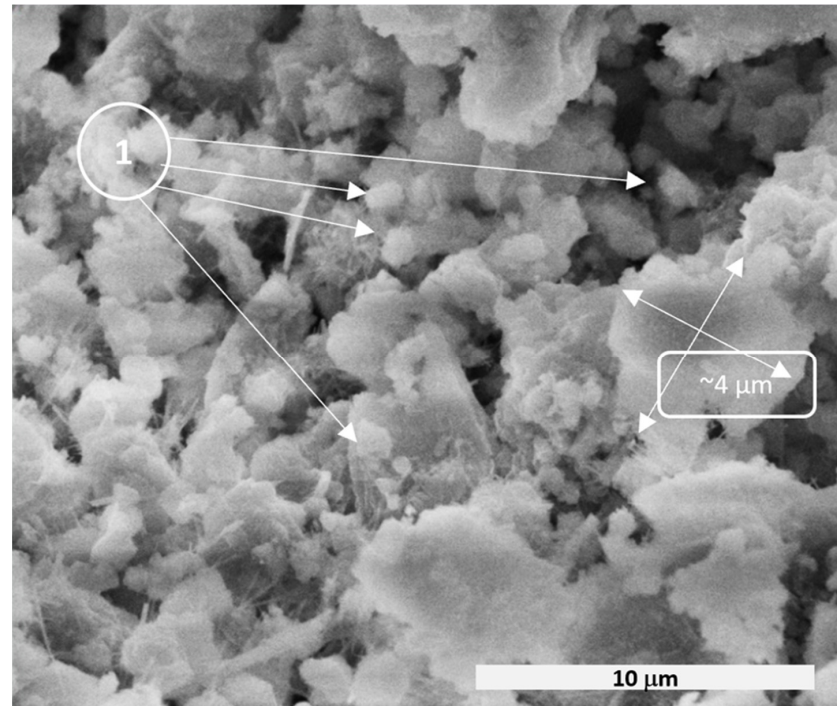


Figure 11. SEM image of the sample surface with an indication of different crystal forms.

Figure 11 illustrates, as in Figure 10, that the crystals are of comparable size and fairly evenly distributed, which is to be expected since they have the same amounts of lime and cement as in the previous case.

Regarding the relative elemental composition measured with EDS presented in Figures 12–14, it is easily observable that the percentage of Ca increased significantly in sample 16 compared to the other samples as the amount of lime added increased. The EDS spectra indicate the major elements of O, Ca, Si, and Na in the hemp concrete sample, as shown in Figures 12–14, with values between 39.71% for sample 16 and 62.40% for sample 3 (Table 9). Values for Ca range from 23.32% for sample 3 to 55%; 27.42% for sample 8 (Table 10) or 63% for sample 16 (Table 11).

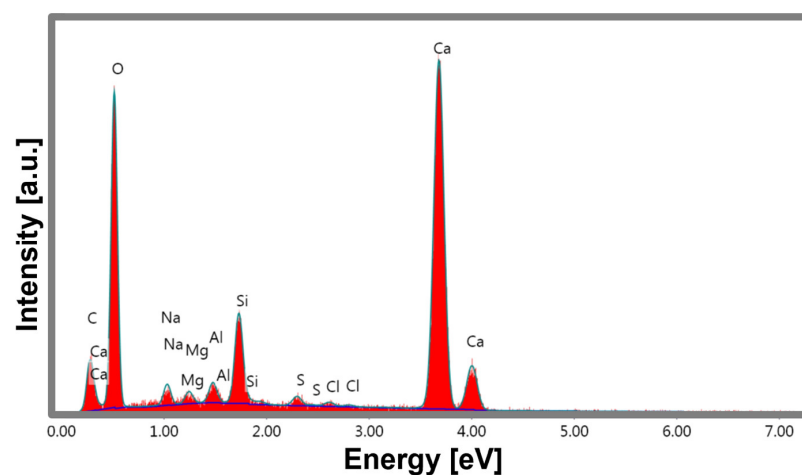


Figure 12. EDS spectrum for sample 3.

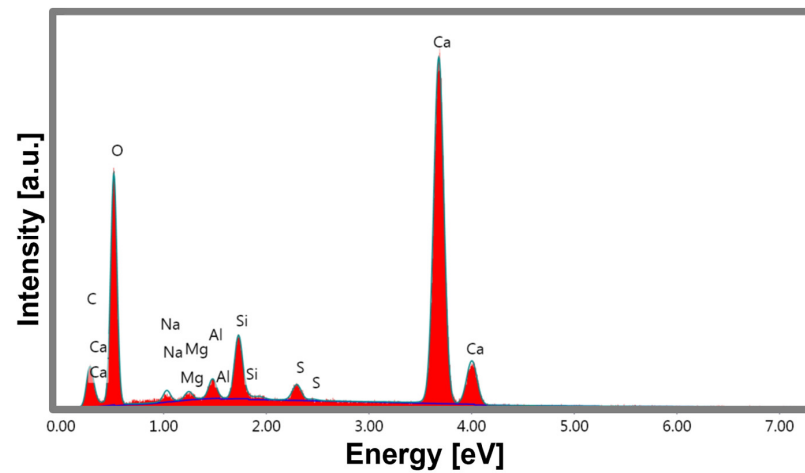


Figure 13. EDS spectrum for sample 8.

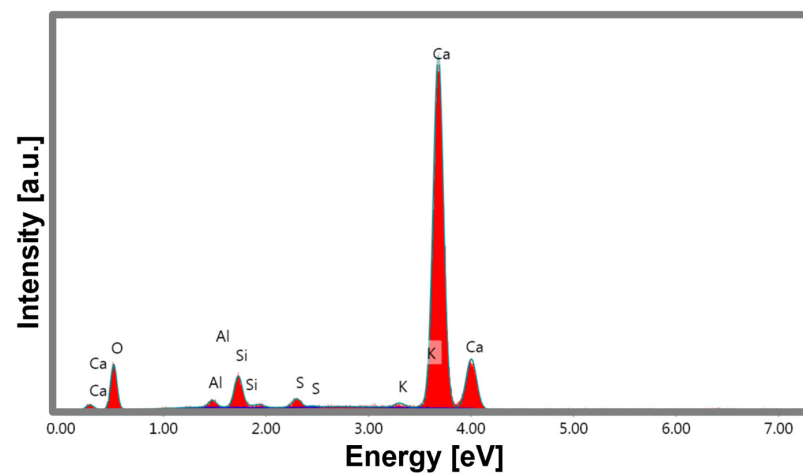


Figure 14. EDS spectrum for sample 16.

Table 9. Relative elemental composition of hemp concrete for sample 3.

	Element	Weight %
1	C	6.31
2	O	62.40
3	Na	2.41
4	Mg	0.71
5	Al	0.90
6	Si	3.44
7	S	0.34
8	Ca	23.32

Table 10. Relative elemental composition of hemp concrete for sample 8.

	Element	Weight %
1	C	5.53
2	O	60.29
3	Na	1.56
4	Mg	0.57
5	Al	1.04
6	Si	2.87
7	S	0.71
8	Ca	27.42

Table 11. Relative elemental composition of hemp concrete for sample 16.

	Element	Weight %
1	O	39.71
2	Al	0.72
3	Si	2.79
4	S	0.73
5	K	0.42
6	Ca	55.63

4. Conclusions

The validation results demonstrated the usefulness of the advanced DoE method in optimising the physical and mechanical performance of hemp concrete. Improvements in compressive strength up to 0.635 MPa and a reduction in the heat transfer coefficient of up to 0.1021 W/m²*K were obtained, demonstrating that the method used can provide a tool capable of optimising the performance of sustainable hemp-based concrete according to a user's requirements.

The parametric optimisation used in this work has facilitated finding the configurations necessary to obtain the physicochemical characteristics desired by the user. In addition, the equations obtained allow us to make predictions in the field of analysis domain for any combination of parameters that simultaneously satisfy the desired requirements of these materials. Compared to the classical methods of optimisation, which are usually of a single parameter, and compared to trial and error, the experimental planning method is an advanced method of planning, analysis and optimisation that helps the user to achieve the proposed objectives with minimum effort and maximum information. The method used in the study allows the analysis and design of construction materials using as variable parameters other elements, such as magnesium oxide, hydraulic lime, polyester resins, etc.

An advantage is given by the possibility of an advanced analysis of the influence that these parameters have on the performance of the mixtures obtained. The information obtained allows the development of future studies for the research of other types of binders used to obtain sustainable ecological concrete based on hemp, such as casein, bone glue, cereal starch, or even fungal bacteria.

Author Contributions: Conceptualisation, L.A. and D.L.; methodology, L.A.; software, D.L.; validation, D.L. and L.A.; statistical analysis and optimisation, D.L.; chemical characterisation, L.J.; chemical composition analysis, I.M.; formal analysis, EDAX and SEM investigation, I.M.; SEM interpretation, L.J.; material characterisation, SEM interpretation, I.R. and I.M.; resources, R.D.B.; writing—original draft preparation, L.A. and D.L.; writing—review and editing, L.A.; supervision, D.L. All authors have read and agreed to the published version of the manuscript.

Funding: This research received no external funding.

Institutional Review Board Statement: Not applicable.

Informed Consent Statement: Not applicable.

Data Availability Statement: Not applicable.

Conflicts of Interest: The authors declare no conflict of interest.

References

1. Di Capua, S.E.; Paolotti, L.; Moretti, L.; Rocchi, L.; Boggia, A. Evaluation of the Environmental Sustainability of Hemp as a Building Material, through Life Cycle Assessment. *Environ. Clim. Technol.* **2021**, *25*, 1215–1228. [[CrossRef](#)]
2. Stevulova, N.; Cigasova, J.; Schwarzova, I.; Sicakova, A.; Junak, J. Sustainable bio-aggregate-based composites containing hemp hurds and alternative binder. *Buildings* **2018**, *8*, 25. [[CrossRef](#)]
3. Bledzki, A.K.; Gassan, J. Composites reinforced with cellulose based fibres. *Progress Polym. Sci.* **1999**, *24*, 221–274. [[CrossRef](#)]

4. Barbhuiya, S.; Bhusan Das, B. A Comprehensive review on the use of hemp in concrete. *Constr. Build. Mater.* **2022**, *341*, 127857. [[CrossRef](#)]
5. Sahmenko, G.; Sinka, M.; Namsone, E.; Korjakins, A.; Bajare, D. Sustainable Wall Solutions Using Foam Concrete and Hemp Composites. *Environ. Clim. Technol.* **2021**, *25*, 917–930. [[CrossRef](#)]
6. Antony, S.; Cherouat, A.; Montay, G. Fabrication and Characterization of Hemp Fiber Based 3D Printed Honeycomb Sandwich Structure by FDM Process. *Appl. Compos. Mater.* **2020**, *27*, 935–953. [[CrossRef](#)]
7. Sinka, M.; Spurina, E.; Korjakins, A.; Bajare, D. Hempcrete—CO₂ Neutral Wall Solutions for 3D Printing. *Environ. Clim. Technol.* **2022**, *26*, 742–753. [[CrossRef](#)]
8. Memari, A.M.; Zuabi, W. Review of Hempcrete as a Sustainable Building Material. *Int. J. Archit. Eng. Constr.* **2021**, *10*, 1–17. [[CrossRef](#)]
9. Preikss, I.; Skujans, J.; Adamovics, A.; Iljins, U. Evaluation of hemp (*Cannabis sativa* L.) quality parameters for building material from foam gypsum products. *Chem. Eng. Trans.* **2013**, *32*, 1639–1643.
10. Arizzi, A.; Brümmer, M.; Martin-Sánchez, I.; Cultrone, G.; Viles, H. The influence of the type of lime on the hygric behavior and bio-receptivity of hemp lime composites used for rendering applications in sustainable new construction and repair works. *PLoS ONE* **2015**, *10*, e0125520. [[CrossRef](#)]
11. Karade, S.R. Cement-bonded composites from lignocellulosic wastes. *Constr. Build. Mater.* **2010**, *24*, 1323–1330. [[CrossRef](#)]
12. Hamšik, P.; Král, P. Composite materials from hemp and hydraulic lime for use in building and wood-constructions. *Wood Res.* **2014**, *59*, 871–882.
13. Archila Santos, H.; Pesce, G.; Ansell, M.; Ball, R. Limeboo: Lime as a Replacement for Cement in Wall-Framing Systems with Bamboo-Guadua (Bahareque Encementado). In Proceedings of the 16th International Conference on Non-Conventional Materials and Technologies (NOCMAT 2015), Winnipeg, MB, Canada, 10–13 August 2015. [[CrossRef](#)]
14. Sardar, S.S.; Hozan, L.R. Using Hemp for Walls as a Sustainable Building Material. *JSSE* **2022**, *24*, 1323–1330. [[CrossRef](#)]
15. Manzi, S.; Sassoni, E.; Motori, A.; Montecchi, M.; Canti, M. New composite with hemp hurds for sustainable buildings. *Environ. Eng. Manag. J.* **2013**, *12*, 31–34.
16. Sudarshan, D.K.; Sudarsan, J.S. Hemp concrete: A sustainable green material for conventional concrete. *J. Build. Mater. Sci.* **2021**, *3*, 3189. [[CrossRef](#)]
17. Faiz Ahmed, A.T.M.; Islam, M.Z.; Mahmud, M.S.; Sarker, M.E.; Islam, M.R. Hemp as a potential raw material toward a sustainable world: A review. *Heliyon* **2022**, *8*, e08753. [[CrossRef](#)]
18. Schluttenhofer, C.; Yuan, L. Challenges towards Revitalizing Hemp: A multifaceted Crop. *Trends Plant Sci.* **2017**, *22*, 917–929. [[CrossRef](#)]
19. Viswanathan, M.B.; Cheng, M.-H.; Clemente, T.E.; Dweikat, I.; Singh, V. Economic perspective of ethanol and biodiesel coproduction from industrial hem. *J. Clean. Prod.* **2021**, *299*, 126875. [[CrossRef](#)]
20. Dahal, R.K.; Acharya, B.; Dutta, A. Mechanical, Thermal, and Acoustic Properties of Hemp and Biocomposite Materials: A Review. *J. Compos. Sci.* **2022**, *6*, 373. [[CrossRef](#)]
21. Parcesepe, E.; De Masi, R.F.; Lima, C.; Mauro, G.M.; Pecce, M.R.; Maddaloni, G. Assessment of Mechanical and Thermal Properties of Hemp-Lime Mortar. *Materials* **2021**, *14*, 882. [[CrossRef](#)]
22. Curto, D.; Guercio, A.; Franzitta, V. Investigation on a Bio-Composite Material as Acoustic Absorber and Thermal Insulation. *Energies* **2020**, *13*, 3699. [[CrossRef](#)]
23. Pochwała, S.; Makiola, D.; Anweiler, S.; Böhm, M. The Heat Conductivity Properties of Hemp–Lime Composite Material Used in Single-Family Buildings. *Materials* **2020**, *13*, 1011. [[CrossRef](#)] [[PubMed](#)]
24. Ntimugura, F.; Vinai, R.; Harper, A.; Walker, P. Mechanical, thermal, hygroscopic and acoustic properties of bio-aggregates—Lime and alkali—Activated insulating composite materials: A review of current status and prospects for miscanthus as an innovative resource in the South West of England. *Sustain. Mater. Technol.* **2020**, *26*, e00211. [[CrossRef](#)]
25. Pietruszka, B.; Gołębiewski, M.; Lisowski, P. Characterization of Hemp-Lime Bio-Composite. *IOP Conf. Ser. Earth Environ. Sci.* **2019**, *290*, 012027. [[CrossRef](#)]
26. Bayraktar, O.Y.; Tobbala, D.E.; Turkoglu, M.; Kaplan, G.; Tayeh, B.A. Hemp fiber reinforced one-part alkali-activated composites with expanded perlite: Mechanical properties, microstructure analysis and high-temperature resistance. *Constr. Build. Mater.* **2023**, *363*, 129716. [[CrossRef](#)]
27. Demir, I.; Doğan, C. Physical and Mechanical Properties of Hempcrete. *Open Waste Manag. J.* **2020**, *13*, 26–34. [[CrossRef](#)]
28. Delhomme, F.; Hajimohammadi, A.; Almeida, A.; Jiang, C.; Moreau, D.; Gan, Y.; Wang, X.; Castel, A. Physical properties of Australian hurd used as aggregate for hemp concrete. *Mater. Today Commun.* **2020**, *24*, 100986. [[CrossRef](#)]
29. Novakova, P.; Sal, J. Use of technical hemp for concrete—Hempcrete. *Mater. Sci. Eng.* **2019**, *603*, 052095. [[CrossRef](#)]
30. Tarun, J.; Karade, S.R.; Singh, L.P. A review of the properties of hemp concrete for green building applications. *J. Clean. Prod.* **2019**, *239*, 117852. [[CrossRef](#)]
31. Seng, B.; Magniont, C.; Lorente, S. Characterization of a precast hemp concrete. Part I: Physical and thermal properties. *J. Build. Eng.* **2019**, *24*, 100540. [[CrossRef](#)]
32. Abdellatef, T.; Khan, M.A.; Khan, A.; Alam, M.I.; Kavgić, M. Mechanical, thermal and moisture buffering properties of novel insulating hemp-lime composite building materials. *Materials* **2020**, *13*, 5000. [[CrossRef](#)]

33. Lawrence, M.; Fodde, E.; Paine, K.; Walker, P. Hygrothermal Performance of an Experimental Hemp-Lime Building. *Key Eng. Mater.* **2012**, *517*, 413–421. [CrossRef]
34. Luthe, T. Mon Viso Institute. Hemp as incubator of a circular economy. *Hanf Mang.* **2019**, *2019*, 61–68.
35. Moscariello, C.; Matassa, S.; Esposito, G.; Papirio, S. From residue to resource: The multifaceted environmental and bioeconomy potential of industrial hemp (*Cannabis sativa* L.). *Resour. Conserv. Recyc.* **2021**, *175*, 105864. [CrossRef]
36. Arehart, J.H.; Nelson, W.S.; Srubar, W.V. On the theoretical carbon storage and carbon sequestration potential of hempcrete. *J. Clean. Prod.* **2020**, *266*, 121846. [CrossRef]
37. Tarun, J.; Kumar, S. Assessment of Carbon Sequestration of Hemp Concrete. In Proceedings of the International Conference on Advances in Construction Materials and Systems, Chennai, India, 3–8 September 2017.
38. Sinka, M.; Korjakins, A.; Bajare, D.; Šahm, G. Bio-based construction panels for low carbon development. *Energy Procedia* **2018**, *147*, 220–226. [CrossRef]
39. Shen, Z.; Tiruta-Barna, L.; Hamelin, L. From hemp grown on carbon-vulnerable lands to long-lasting bio-based products: Uncovering trade-offs between overall environmental impacts, sequestration in soil, and dynamic influences on global temperature. *Sci. Total Environ.* **2022**, *846*, 157331. [CrossRef]
40. Cazacu, C.; Muntean, R.; Galatanu, T.; Daniel, T. Hemp lime technology. *Bull. Trans. Univ. Bras.* **2016**, *9*, 19.
41. Tang, Y.; Wang, Y.; Wu, D.; Liu, Z.; Zhang, H.; Zhu, M.; Chen, Z.; Sun, J.; Wang, X. An experimental investigation and machine learning-based prediction for seismic performance of steel tubular column filled with recycled aggregate concrete. *Rev. Adv. Mater. Sci.* **2022**, *61*, 849–872. [CrossRef]
42. Feng, W.; Tang, Y.; Yang, Y.; Cheng, Y.; Qiu, J.; Zhang, H.; Isleem, H.F.; Tayeh, B.A.; Namdar, A. Mechanical behavior and constitutive model of sustainable concrete: Seawater and sea-sand recycled aggregate concrete. *Constr. Build. Mater.* **2023**, *364*, 130010. [CrossRef]
43. Seidenfeld, T.R.A. *Fisher on the Design of Experiments and Statistical Estimation*; Springer: Berlin/Heidelberg, Germany, 1992; pp. 23–36.
44. Ficher, R.A. Statistical method for research worker. *J. Am. Stat. Assoc.* **1951**, *46*, 51–54.
45. Draper, N.R. *Introduction to Box and Wilson (1951) On the Experimental Attainment of Optimum Conditions. Breakthroughs in Statistics*; Springer Series in Statistics; Springer: New York, NY, USA, 1992. [CrossRef]
46. Ross, P.J. *Taguchi Techniques for Quality Engineering*; McGraw-Hill: New York, NY, USA, 1988.
47. *SR EN 12390-1*; Test on Hardened Concrete. Part 1: Shape, Dimensions and Other Conditions for Specimens and Patterns. Institut za Standardizaciju Srbije: Belgrade, Serbia, 2021.
48. *SR EN 12390-3*; Testing on Hardened Concrete. Part 3: Compressive Strength of Specimens. Institut za Standardizaciju Srbije: Belgrade, Serbia, 2021.
49. Montgomery, D.C. *Design and Analysis of Experiments*, 8th ed.; John Wiley & Sons, Inc.: New York, NY, USA, 2013.
50. Box, G.E.P.; Draper, N. *Empirical Model Building and Response Surfaces*; Wiley: New York, NY, USA, 1987.
51. Box, G.E.P.; Hunter, W.; Hunter, J.S. *Statistics for Experimenters*; Wiley: New York, NY, USA, 1978.
52. Mondal, S.; Naik, S.K.; Haris, A.A.; Mishra, J.S.; Mukherjee, J.; Rao, K.K.; Bhatt, B.P. Effect of conservation tillage and rice-based cropping systems on soil aggregation characteristics and carbon dynamics in Eastern Indo-Gangetic Plain. *Paddy Water Environ.* **2020**, *18*, 573–586. [CrossRef]
53. Bansod, S.P.; Parikh, J.K.; Sarangi, P.K. Pineapple peel waste valorization for extraction of bio-active compounds and protein: Microwave assisted method and Box Behnken design optimization. *Environ. Res.* **2023**, *221*, 115237. [CrossRef] [PubMed]
54. Wei, P.; Yin, G.; Shi, M.; Zhang, W.; Feng, J. Performance investigation and parameter optimization of ultra-light aerated concrete using orthogonal experimental design. *Case Stud. Constr. Mater.* **2023**, *18*, e01841. [CrossRef]
55. Gou, M.; Hou, W.; Zhou, L.; Zhao, J.; Zhao, M. Preparation and properties of calcium aluminate cement with Bayer red mud. *Constr. Build. Mater.* **2023**, *373*, 130827. [CrossRef]
56. Zhang, Q.; Jin, X.; Zhang, F.; Yuan, H.; Zhou, B. Equivalent modeling and multi-parameter coupling optimization for DFIG-based wind farms considering SSO mode. *Front. Energy Res.* **2023**, *10*, 1097185. [CrossRef]
57. Yang, S.; Zhou, D.; Wang, Y.; Li, P. Comparing impact of multi-factor planning layouts in residential areas on summer thermal comfort based on orthogonal design of experiments (ODOE). *Build. Environ.* **2020**, *182*, 107145. [CrossRef]
58. Adeyinka, S.; Yusuff, A.K.; Bhonsle, D.P.; Bangwal, N.A. Development of a barium-modified zeolite catalyst for biodiesel production from waste frying oil: Process optimization by design of experiment. *Renew. Energy* **2021**, *177*, 1253–1264. [CrossRef]
59. Sivasubramanian, J.; Gino, Y. Effect of sodium silicate on hardening property of concrete. *Int. J. Civ. Eng. Tech.* **2019**, *10*, 642–650.
60. Isomet Manual. Available online: https://www.appliedp.com/download/manual/isomet2114 Ug_en.pdf (accessed on 21 October 2022).

Disclaimer/Publisher's Note: The statements, opinions and data contained in all publications are solely those of the individual author(s) and contributor(s) and not of MDPI and/or the editor(s). MDPI and/or the editor(s) disclaim responsibility for any injury to people or property resulting from any ideas, methods, instructions or products referred to in the content.